Title	Band and scattering tuning for high performance thermoelectric Sn1-xMnxTe alloys
Author(s)	Li, W; Chen, ZW; Lin, SQ; Chang, YJ; Ge, BH; Chen, Y; Pei, YZ
Citation	Journal of Materiomics, 2015, v. 1 n. 4, p. 307-315
Issued Date	2015
URL	http://hdl.handle.net/10722/229249
Rights	This work is licensed under a Creative Commons Attribution-NonCommercial-NoDerivatives 4.0 International License.

Available online at www.sciencedirect.com

ScienceDirect

J Materiomics 1 (2015) 307–315

www.ceramsoc.com/en/

www.journals.elsevier.com/journal-of-materiomics/

Band and scattering tuning for high performance thermoelectric $Sn_{1-x}Mn_xTe$ alloys

Wen Li [a], Zhiwei Chen [a], Siqi Lin [a], Yunjie Chang [b], Binghui Ge [b], Yue Chen [c], Yanzhong Pei [a,*]

[a] *Key Laboratory of Advanced Civil Engineering Materials of Ministry of Education, School of Materials Science and Engineering, Tongji Univ., 4800 Caoan Rd., Shanghai 201804, China*

[b] *Beijing National Laboratory for Condensed Matter Physics, Institute of Physics, Chinese Academy of Science, Beijing 100190, China*

[c] *Department of Mechanical Engineering, The University of Hong Kong, Pokfulam Road, Hong Kong SAR, China*

Received 15 September 2015; revised 16 September 2015; accepted 17 September 2015
Available online 9 October 2015

Abstract

The thermoelectric figure of merit zT of SnTe, an analogue to PbTe, has long been known to be about 0.6, mainly due to its single band transport behavior. Similar to what has been found in PbTe, alloying with group II monotellurides such as CdTe, HgTe, MgTe enables a reduced energy separation between the two valence bands of SnTe, leading to converged bands for a significantly increased zT to ~1.1 with demonstrated further improvements by other independent strategies such as nanostructuring. Here we show alloying with highly soluble MnTe not only tunes the band structure but also reduces the lattice thermal conductivity, leading to a record zT of ~1.3 at 900 K in the alloy form that does not rely on additional mechanisms for lattice thermal conductivity reduction. This work demonstrates $Sn_{1-x}Mn_xTe$ as a potential alternative for PbTe with toxic Pb.

Keywords: SnTe; Thermoelectric; Alloying; Band engineering; Phonon scattering

1. Introduction

Thermoelectric (TE) energy conversion technique, convert heat into electricity directly based on the Seebeck effects, has been utilized for powering the spacecrafts of deep-space missions for decades [1]. In recent years, TE application have attracted increasing interest to the automotive industry as a sustainable and emission free route to vehicular waste heat recovery [2], however, the relatively low conversion efficiency limits the widespread use. The conversion efficiency of a TE material is determined by the figure of merit, $zT = S^2\sigma T/(\kappa_e + \kappa_L)$, where S, σ, κ_e and κ_L are the Seebeck coefficient, electrical conductivity, and the electronic and lattice components to the thermal conductivity, respectively. To maximize zT, high S, highσ, and low $\kappa_e + \kappa_L$ are required, but the interdependence between S, σ and κ_L *via* the carrier concentration in a TE material makes the property manipulation difficult [3].

The only one independent material property is the lattice thermal conductivity, which needs to be minimized. A variety of strategies such as nanostructuring [4–13], lattice anharmonicity [14,15] and liquid phonons [16,17], are proposed to achieve high performance TE materials through a low lattice thermal conductivity, which have demonstrated in various materials over the recent ~15 years. For example, through the all scale microstructure engineering in p-PbTe to scatter heat-carrying phonons with a broad wavelength, $zT > 2$ is reported [5].

Unfortunately, it is well believed in bulk materials at least there is a lower limit to the lattice thermal conductivity when the phonon mean free path reaches the interatomic distance [18]. Most of the reported high zT PbTe materials actually show a lattice thermal conductivity approaching this lower

* Corresponding author.
E-mail address: yanzhong@tongji.edu.cn (Y. Pei).
Peer review under responsibility of The Chinese Ceramic Society.

http://dx.doi.org/10.1016/j.jmat.2015.09.001

boundary [7]. Recently, a concept from the other aspect, of band engineering [19,20] to increase the thermoelectric power factor ($S^2\sigma$) and therefore zT, has also been proven to be successful. Demonstrated strategies are typified by the high band degeneracy through band convergence in PbTe [21], Mg_2Si [22,23] and half-Heusler [3,24] alloys, and by the resonant doping [20,25–28].

The concept of band convergence is usually demonstrated in solid solutions. Taking p-type PbTe as an example, alloying with PbSe [21], MnTe [29], MgTe [30] and CdTe [31] not only tune the band structure for a high band degeneracy and therefore power factor, but also scatter phonon for a decreased lattice thermal conductivity (κ_L), leading to a significant enhancement on TE performance [21,29–31]. The band convergence is achievable, first of all, due to the existence of two sub-valence bands in PbTe with a small energy offset ($\Delta E = 2–4\ k_BT$) at room temperature [32–37], in addition, the formation of solid solutions with these species enable a reduced energy offset between these two bands [19]. The reduction on the lattice thermal conductivity can be well understood based on the Debye–Callaway model [38–40], where the alloy defects lead to a phonon scattering due to the mass and strain fluctuations between the host and guest atoms. A combination of band convergence and alloy defects scattering effects, PbTe alloys show an extraordinary high zT value of ~1.8 [21,30,31] without relying on the nanostructuring [4–13], lattice anharmonicity [14,15] or liquid phonons [16,17] mechanisms, leading to a great potential for further improvements through a panoscopic approach [5,41,42].

Due to the above well demonstrated strategies for high zT in PbTe, as an analogue to PbTe, lead-free tin telluride (SnTe) can also be expected to achieve a high thermoelectric performance as an environmental friendly alternative to PbTe. SnTe has the same crystal structure and a similar electronic band structure with PbTe. The biggest difference is the energy offset (ΔE) between the two sub-valence bands in SnTe ($\Delta E = 12–15\ k_BT$) [43] being significantly larger than that of PbTe ($\Delta E = 2–4\ k_BT$) at room temperature [44–46]. The large difference on valence band offset leads to completely different transport properties of holes between PbTe and SnTe. In the case of p-PbTe, when the material is optimally doped to have a room temperature Hall carrier concentration (n_H) of $5–20 \times 10^{19}$ cm^{-3} or higher, the carriers inherently populate the lower valence band enables a high zT to be achieved because of the overall higher band degeneracy. However, SnTe has only one valence band contributing to the thermoelectric transport properties at these carrier concentrations, which actually limits the maximal zT to be ~0.6 [47]. Further increased carrier concentration to ~10^{21} cm^{-3}, leading the Fermi level deeper into the first valence band, indeed resulting a redistribution of holes from the first to the second valence band. Unfortunately, these carrier concentrations are overwhelmingly higher than what is needed for optimized zT can be achieved. This leads to the net fact that thermoelectric SnTe practically acts as single band transport behavior [47].

It is then straight forward that a great enhancement on zT can be expected in SnTe if the valence band offset is reduced. Very similar to the case of PbTe [29–31], formation of SnTe solid solution with group II monotellurides such as MgTe [48], CdTe [49] and HgTe [50], has been very recently proved to effectively reduce the valence band offset. The resulting effects of band convergence and phonon scattering by alloy defects in solid solutions, leads to a significantly increased zT to ~1.1 [26]. Taking solid solutions as a starting point, a combination with other strategies such as nanostructuring [26,49,51] and resonant doping [26] enables a further thermoelectric performance enhancement [26,49,50].

The solubility of reported group II monotellurides (Cd, Hg, Mg) in SnTe, which enables a band convergence, is less than 10%. Providing the room temperature valance band offset ($12–15\ k_BT$) in SnTe [43] is much larger than that in PbTe ($2–4\ k_BT$) [44–46], highly soluble species is expected to allow the band structure to be engineered in a larger degree. Additionally, higher concentration of solute, particularly having large atomic mass difference with the solvent, will lead to a stronger phonon scattering by alloy defects.

According to the phase diagram [52], highly soluble MnTe is used to form solid solution with SnTe in this work. We confirmed its high solubility (~15% mol) and its effectiveness on converging the valence bands in SnTe. Further due to the resulting phonon scattering by alloy defects, a significantly enhanced thermoelectric figure of merit, zT~1.3 is obtained, being the highest in the solid solution form ever reported [26,27,48–50]. Different from other high thermoelectric performance SnTe materials reported so far, the obtained high zT in this work does not rely on any other strategies for a further reduction on the lattice thermal conductivity, demonstrating $Sn_{1-x}Mn_xTe$ solid solutions as a superior starting material for further improvements.

2. Experimental procedure

Polycrystalline $Sn_{1-x}Mn_xTe$ alloys with x up to 0.18 were synthesized by melting the stoichiometric amount of high purity elements (>99.99%) at 1123 K for 6 h, quenching in cold water and annealing at 950 K for 3 days. I-doping within 2% was used to tune the carrier concentration for the samples with $x = 0.15$. The resulting ingots were hand ground into fine powder for X-ray diffraction (XRD, Dandong Haoyuan Instrument Co. LTD) and hot press. Pellet samples were obtained by an induction heating hot press system [53] at 900 K for 30 min under a uniaxial pressure of ~60 Mpa. The obtained dense samples (>98% of the theoretical density) were about 12 mm in diameter and ~1.5 mm in thickness. To be less involved in measurement uncertainties due to the possible hysteresis and the sample dimension determinations, the electrical transport properties including resistivity, Seebeck coefficient and Hall coefficient were simultaneously measured on the pellet samples during both heating and cooling. The Seebeck coefficient was obtained from the slope of the thermopower vs. temperature gradients within 0–5 K [54]. The resistivity and Hall coefficient (R_H) were measured using the van der Pauw technique under a reversible magnetic field of 1.5 T. Thermal diffusivity (D) was measured using a laser flash

technique with the Netzsch LFA457 system, the heat capacity was determined by $C_p(k_B/\text{atom}) = [3.07 + 0.00047(T/\text{K-}300)]$ [19,21,29–31,55–57], where T is the absolute temperature. It should be emphasized that this simple equation is obtained by fitting the experimental data reported by Blachnik with an uncertainty of 5% for all the lead chalcogenides and tin telluride [58]. The thermal conductivity was calculated *via* $\kappa = dC_pD$, where d is the density measured using the mass and geometric volume of the pellet. The sound velocity was measured using an ultrasonic pulse-receiver (Olympus-NDT) equipped with an oscilloscope (Keysight). All the transport property measurements were carried out under vacuum in the temperature range of 300–900 K. The measure uncertainty for each transport property (S, σ and κ) is about 5%. The microstructure was characterized by High-Angle Annular Dark Field (HAADF) imaging in Scanning Transmission Electron Microscopy (STEM) mode. STEM specimens were prepared by mechanical slicing, polishing, and dimpling, and followed by ion-milling with liquid nitrogen until electron transparency was achieved.

The electronic band structures were computed within the framework of density functional theory (DFT) which was carried out using the Perdew-Burke-Ernzerhof (PBE) parametrization of the generalized gradient approximation (GGA) [59] as implemented in the Vienna ab initio simulation package (VASP) [60,61]. We adopted a 3 × 3 × 3 supercell of $Sn_{27}Te_{27}$ with and without Mn substitution on the Sn site. In the case of $MnSn_{26}Te_{27}$, we do not have to consider the Mn-occupation configuration because all the Sn atoms in this supercell are equivalent. When Mn-concentration increases to $Mn_2Sn_{25}Te_{27}$, we have considered three atomic configurations where the substitutional Mn atom pairs are in the first to the third nearest neighbors in the Sn sub-lattice. A plane wave energy cutoff of 350 eV was applied to all of the $Sn_{1-x}Mn_xTe$ systems, and charge self-consistency was performed until the energy was converged to within 10^{-6} eV. A k-point mesh of 4 × 4 × 4 was generated by the Monkhorst-Pack scheme [62] for the 3 × 3 × 3 supercell of the rock-salt structure containing 54 atoms. All the systems were fully relaxed before the non-self-consistent band structure calculations, and the spin-orbit coupling effects were included.

3. Results and discussion

The XRD patterns of $Sn_{1-x}Mn_xTe$ ($x = 0$, 0.03, 0.06, 0.09, 0.12, 0.15, 0.18) samples are shown in Fig. 1a. All the peaks can be well indexed to the rock-salt structure as $x \leq 0.15$, indicating single phase of all samples. With a further increase in x to 0.18, impurity phase is observed, which can be indexed to MnTe phase. Importantly, the lattice parameter (a) is found to decrease linearly with the increasing x up to 0.15 *via* da/dx = 0.44 Å/mol% (Fig. 1b), following well with the Vegard's law giving an extrapolated lattice parameter of 5.89 Å for MnTe in the rock-salt phase, which is well consistent with that of MnTe obtained from Ca–Mn chalcogenides experimental results (5.88 Å) [63]. The lattice shrinkage can be understood by the smaller size of Mn as compared with Sn. Therefore, the solubility of MnTe in SnTe is estimated to be about 15% mol., which is in good agreement with the literature [52]. Due to the much inferior thermoelectric performance of the two-phase sample with x = 0.18, its transport properties are not shown in the following discussion for clarity.

To further confirm the formation of solid solution, $Sn_{0.85}Mn_{0.15}Te$ sample, the highest Mn concentration in this study, was characterized by HAADF imaging. No secondary phase is observed. A uniformly distributed Mn atoms can be concluded in general, according to our STEM observations. However, some Mn-rich domains with size of ~1 nm are observed, which is identified using Electron Energy Loss Spectroscopy (EELS) technique as shown in Fig. 1c and d. Being the same with the matrix SnTe, these domains crystalize a sodium-chloride structure. The resulting lattice distortion is negligible as evidenced by the high-resolution HAADF observation (Fig. 1d), indicating the single phase of the material. All these results indicate the formation of a solid solution with a MnTe solubility up to ~15 mol%.

Alloying SnTe with MnTe is expected to decrease the energy separation of the two valence bands of SnTe. This is confirmed by our DFT calculations as shown in Fig. 2. The direct band gap and the energy offset between the valence bands (VB) maxima along the Σ direction and at the L point, are found to be 0.1 eV and 0.25 eV for pristine SnTe, respectively. Our calculations are in good agreement with the literature [45,50]. Most importantly, the energy offset between the VB maxima decreases linearly with increasing Mn concentration. Similar band offset reduction due to alloying have also been reported previously [48–50].

The convergence of the two valence bands of SnTe, occurs at ~700 K, has been reported based on the temperature dependent Hall coefficient measurements [64,65]. This is confirmed in Fig. 3a where the temperature dependent R_H for $Sn_{1-x}Mn_xTe$ is shown. It is well believed that a peak R_H will be observed due to the redistribution of carriers between the light- and heavy-hole bands [66]. Therefore, the maximum of R_H, a sign of band convergence [30], appears at a much lower temperature when MnTe concentration increases, indicating the reduction of energy separation between the two valence bands in SnTe due to alloying with MnTe [30]. This is consistent with our band structure calculations.

As can be expected from the resulting redistribution of holes between the two valence bands, the overall Hall mobility should be reduced because the effective mass of the heavy band is much larger than that of the light band [67,68]. This is shown in Fig. 3b. However, the Hall mobility (μ_H) for all the samples show a very similar decrease with increasing temperature *via* $\mu_H \sim T^p$, where $p < -1.5$ [32] indicates an unchanged dominant mechanism of charge carriers scattering by acoustic phonons. Other scattering mechanisms such as by grain boundaries, point defects, polar-optical phonons, and ionized impurities predict $p \geq -0.5$ implying that these mechanisms do not dominate the transport properties. Therefore, the Hall mobility is decreased with increasing MnTe concentration, due to not only the carrier scattering by alloy defects but also the increased less-mobile holes

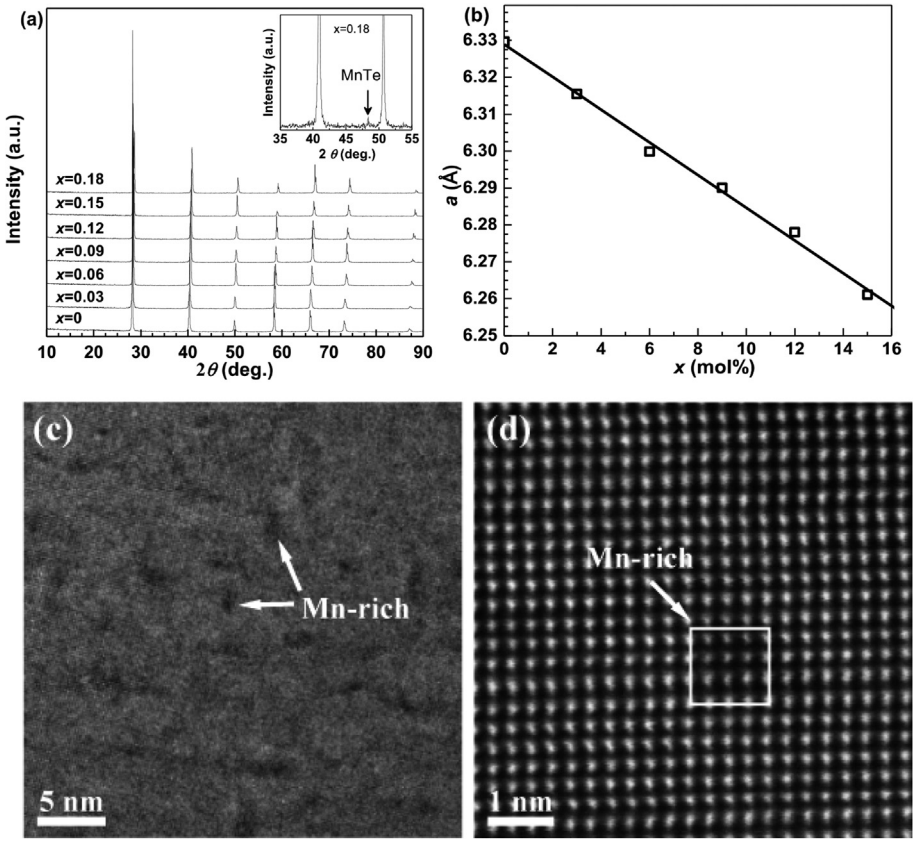

Fig. 1. (a) XRD patterns and (b) the lattice parameter for $Sn_{1-x}Mn_xTe$ ($0 < x < 0.18$), showing a lattice shrinkage and a solubility of ~15% mol can be estimated. (c) Low-magnification and (d) high-resolution HAADF images for $Sn_{0.85}Mn_{0.15}Te$, indicating a formation of solid solution.

residing in the heavy valence band caused by the band convergence.

Because of the redistribution of holes into the heavy valence band, a significant increase in Seebeck coefficient is commonly observed in PbTe [29–31] and SnTe-based alloys [26,27,48–50]. As shown in Fig. 4a, Seebeck coefficient enhancements at room temperature can only be observed in binary SnTe at high Hall carrier concentrations of $n_H > \sim 2 \times 10^{20}$ cm^{-3}, with a maximum appears at $n_H \sim 8 \times 10^{20}$ cm^{-3} [47]. Due to the band convergence effect induced by alloying with MnTe as evidenced from our DFT calculations, it is clearly shown that a higher MnTe concentration leads to a stronger Seebeck coefficient enhancement. This result provides a clear evolution on solid solution reducing the band offset in SnTe, and shows a good agreement with the above mentioned temperature dependent Hall coefficient measurements (Fig. 3a). Furthermore, when back dope the $Sn_{0.85}Mn_{0.15}Te$ solid solution with iodine to obtain different carrier concentrations [47,69], all the resulting materials show a Seebeck coefficient well above the Pisarenko line (Hall carrier concentration dependent Seebek coefficient) that predicted based on a two band model [47]. More quantitatively, the obtained room temperature Seebeck coefficient of ~60 μV/K in $Sn_{0.85}Mn_{0.15}Te$ alloys, is about four times increased as compared with SnTe (~15 μV/K). Fig. 4a also shows a detailed comparison on the Seebeck coefficient with available literatures in SnTe solid solution with band convergence effect. It is shown the Seebeck coefficient enhancement obtained in $Sn_{0.85}Mn_{0.15}Te$ is much more significant than any other ever reported, suggesting a better band alignment that can be expected from the higher solubility of MnTe (~15%). This band convergence resulted Seebeck coefficient enhancement persists to higher temperatures as shown in Fig. 4b.

Because of the reduced band offset between the light and heavy valence bands in $Sn_{1-x}Mn_xTe$ alloys, the resulting more holes residing in the heavy band, contribute much less to the total electrical conductivity. An expected reduction on the overall Hal mobility is usually found in PbTe alloys [29,30], which is confirmed here as well in $Sn_{1-x}Mn_xTe$ alloys, as shown in Fig. 4c and d for both low and high temperatures, respectively. In addition, the alloy defects should lead to local potential energy fluctuations that reduces the mobility [70–72], which has been observed in our previous work on PbTe alloys [29,30]. The Hall mobility reduction is found to be increased with increasing MnTe concentration.

It is the thermoelectric power factor ($PF = S^2\sigma$) that relates to the thermoelectric figure of merit (zT) in a more straight forward way. As shown in Fig. 4e and f for both low and high temperatures, respectively, the power factor is indeed enhanced, which can be well expected from the converged sub-valence bands as indicated by our band structure calculations. Similar behavior has also been obtained in our

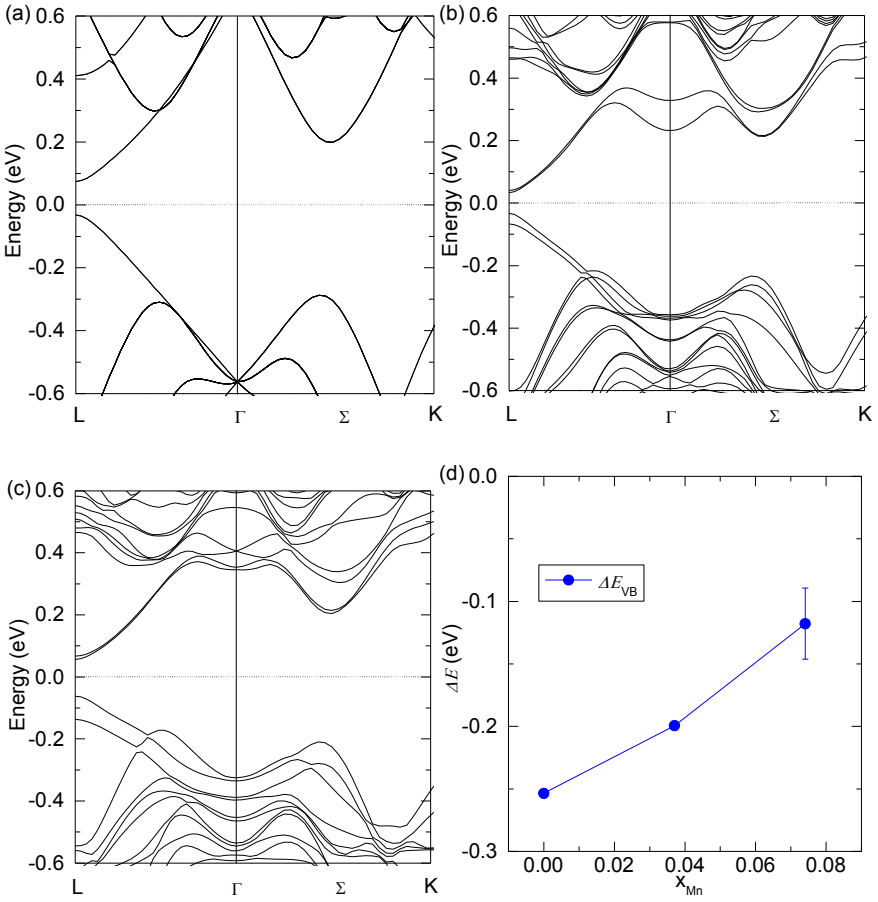

Fig. 2. The calculated band structures for (a) $Sn_{27}Te_{27}$, (b) $Sn_{26}MnTe_{27}$ and (c) $Sn_{25}Mn_2Te_{27}$. (d) The energy offset between the valence band maxima along the Σ direction and at the L point. Three different substitution configurations for $Sn_{25}Mn_2Te_{27}$ have been considered and the average band offset with the resulting error bar is shown in (d).

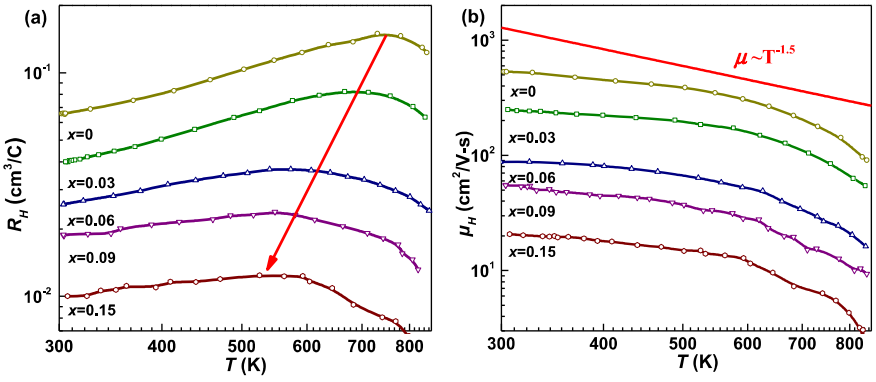

Fig. 3. Temperature dependent (a) Hall coefficient (R_H) and (b) Hall mobility (μ_H) for $Sn_{1-x}Mn_xTe$, indicating a negligible change on the dominant mechanism on the carrier scattering by acoustic phonons but an obvious band offset reduction between the valence bands evidenced from the much lowered temperatures peaking R_H.

previous work on PbTe alloys [29]. As a second order effect for the electronic transport but very important for potentially enhancing zT, the reduced Hall mobility in these alloys will lead to a less contribution to the total thermal conductivity at a given Hall carrier concentration, resulting in a high zT to be obtainable even without an S-enhancement.

Due to the reduced Hall mobility (see Figs. 3 and 4), the resistivity of $Sn_{1-x}Mn_xTe$ alloys is gradually increased with increasing Mn concentration, as show in Fig. 5a. The samples are labeled by both the alloy concentration x and the room temperature Hall carrier concentrations n_H. It is seen that high carrier ($n_H > 9.6 \times 10^{19}$ cm^{-3}) concentration samples show an

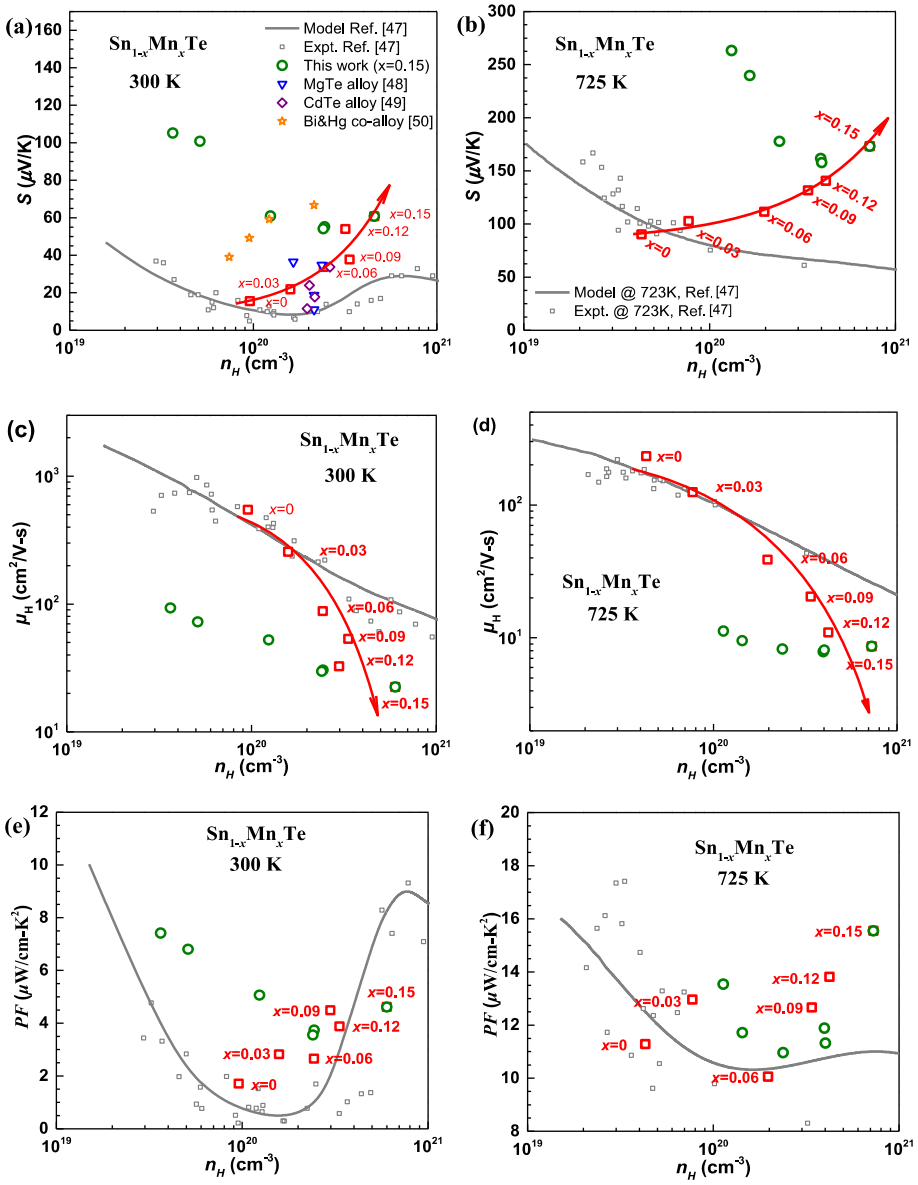

Fig. 4. Hall carrier concentration dependent Seebeck coefficient (a, b), Hall mobility (c, d) and power factor (e, f) at 300 K (a, c, e) and 725 K (b, d, f) for $Sn_{1-x}Mn_xTe$ alloys, with a comparison to the literature [47] modeling and experimental results. The current work (red and green symbols) shows an increase in the Seebeck coefficient, a decrease in the Hall mobility and an enhancement in thermoelectric power factor ($PF = S^2\sigma$).

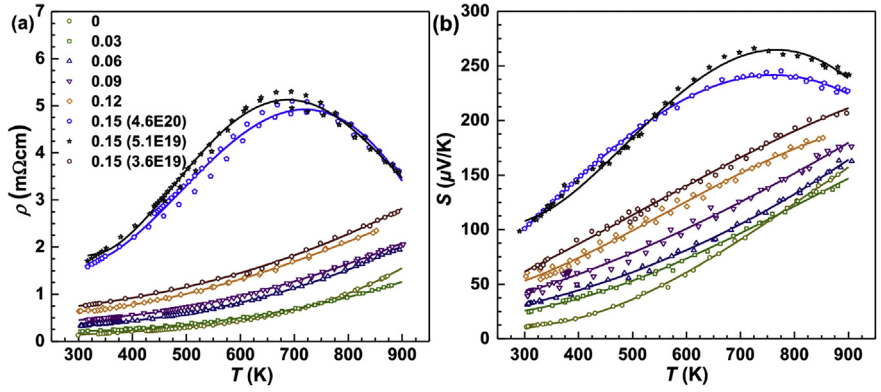

Fig. 5. Temperature dependent resistivity (a) and Seebeck coefficient (b) measured during both heating and cooling for $Sn_{1-x}Mn_xTe$ alloys, indicating a tunable conduction from metallic to intrinsic.

increased resistivity with increasing temperature but low carrier concentration ($n_H < 5.1 \times 10^{19}$ cm^{-3}) samples show an intrinsic conduction at high temperatures.

The temperature dependent Seebeck coefficient is shown in Fig. 5b. Seebeck coefficient for all the samples is positive and consistent with the sign of the Hall coefficient. Importantly, the enhancements on Seebeck coefficient due to the convergence of two valence bands indeed persist to high temperatures. This is well evidenced by the factor that alloys have a much higher Seebeck coefficient even though the Hall carrier concentration is higher than that of binary SnTe. A further decrease in the Hall carrier concentration of $Sn_{0.85}Mn_{0.15}Te$ actually leads to a further enhancement on the Seebeck coefficient. Therefore, the net mechanism for the high temperature *S*-enhancement is neither a carrier concentration nor a carrier scattering change (see Fig. 3b).

Alloying SnTe with MnTe not only converges the valence bands (Fig. 2) for a high thermoelectric power factor, but also significantly reduces the lattice thermal conductivity as shown in Fig. 6. The lattice thermal conductivity is estimated by subtracting the electronic contribution *via* the Wiedemann-Franz law ($\kappa_e = LT/\rho$) from the total thermal conductivity, where L is the Lorenz factor. L is determined using a single parabolic band (SPB) model based on acoustic phonon scattering [73]. While it's a simple model, it has been concluded that this model leads to an uncertainty no more than 10% compared with complicated models, taking both non-parabolic and multiple band effects into account in PbTe [21,65,74] with very similar band structure and unchanged carrier scattering to that of SnTe.

As an important parameter determining the lattice thermal conductivity (κ_L), the sound velocity (v_s) for the samples are measured. It is found that v_s (both longitudinal and transverse branches) does not change more than 5% or show any trend with varying Mn concentration. Therefore, we can exclude the influence of v_s on the lattice thermal conductivity. In fact, the

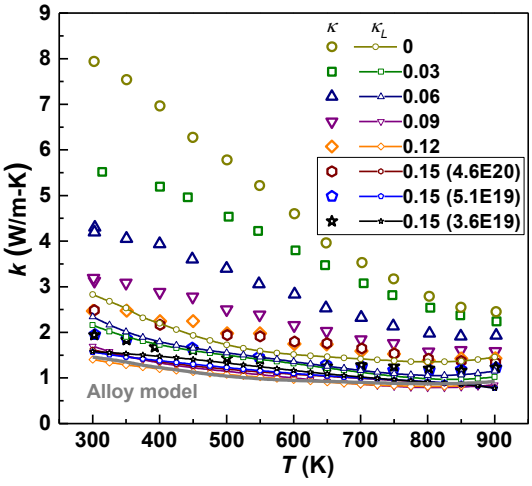

Fig. 6. Temperature dependent total thermal conductivity (κ) and lattice thermal conductivity (κ_L) of $Sn_{1-x}Mn_xTe$ (a). The lattice thermal conductivity reduction due to alloy defects scattering can be well predicted by the Debye–Callaway model (grey solid line).

κ_L-reduction in alloys can be well understood by the Debye–Callaway model, where phonon scattering originates from mass and strain contrasts. Our measured average sound velocities for the longitudinal (3400 m/s) and the transverse (1850 m/s) branches, measured lattice parameter of 6.33 Å, and a lattice anharmonic parameter of 65 (a function of Grüneisen parameter) from literature [75] for PbTe are used for the modeling. The model prediction for alloy with 15% mol. MnTe is given as the grey solid line in Fig. 6. It is seen that the experimental results, for a few different samples with the same MnTe concentration, agree well with our model prediction. It should be noted that, in order to obtain an accurate prediction on κ_L, the model does not have to include the contribution of phonon scattering by the Mn-rich domains as observed by HAADF. This indicates that the Mn-rich domains should not play a significant role on reducing κ_L. Comparing with the amorphous limit of κ_L ~ 0.5 W/m-K estimated for SnTe [18,50] that has been achieved in its alloy with nanostructures [26,49], the lowest κ_L obtained in this work is ~0.8 W/m-K. Therefore, it still remains a possible room for further reduction by other strategies [4–13]. In addition to the reduced κ_L, the observed reduced Hall mobility leads to a higher resistivity and therefore a lower κ_e, resulting a much reduced total thermal conductivity ($\kappa = \kappa_L + \kappa_e$) through alloying.

As shown in Fig. 7a, the combined effects of band engineering for an enhancement on electronic transport properties, and alloy scattering for a reduction on lattice thermal conductivity, successfully lead to a record peak zT of ~1.3 in the form of SnTe alloy. In addition, the average zT in the temperature range studied, is also found to be increased when compared to other SnTe alloys with a similar band convergence effect, as shown in Fig. 7b. It is also shown that the obtained zT_{ave} in this work is much higher than that of SnTe with a resonant doping [26,27]. This high zT_{ave} is actually comparable with that can be achieved in $Sn_{1-x}In_{x/2}Cd_{x/2}Te$ through a dual-strategy including both alloying for band convergence and resonant doping [26], suggesting $Sn_{1-x}Mn_xTe$ alloys as a promising thermoelectric material for high efficiency power generation. The achieved high zT comes largely from the well-enhanced Seebeck coefficient due to the well-aligned bands when heavily alloyed with MnTe up to 15% mol.

4. Summary

Lead-free SnTe, alloyed with MnTe, behaves as an important alternative to thermoelectric PbTe containing toxic Pb. Alloying with MnTe up to 15% mol. engineers not only the bands structure for a power factor enhancement but also the phonon scattering for a lattice thermal conductivity reduction in a favorable manner, which leads to a record peak zT and a superior average zT among literature high performance SnTe in the alloy form. With the well-demonstrated independent strategies such as panosocpic approach for improving thermoelectrics, $Sn_{1-x}Mn_xTe$ retains the availabilities for further increased zT, due to its relatively high lattice thermal conductivity.

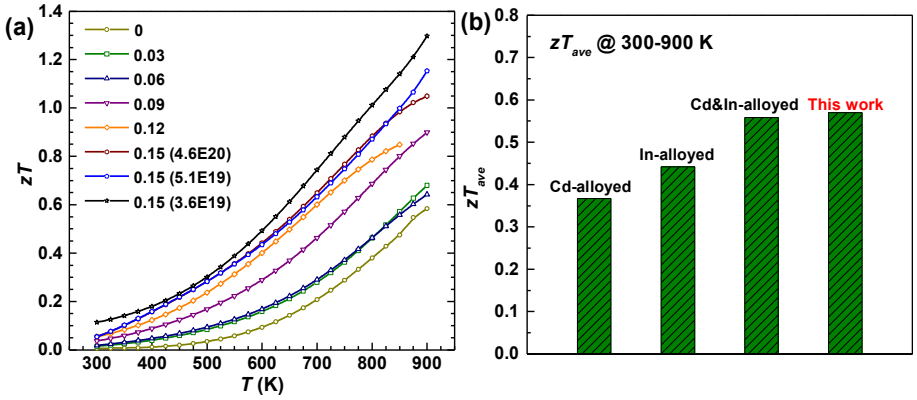

Fig. 7. Temperature dependent thermoelectric figure of merit (a) and its average value (b) between 300 and 900 K for $Sn_{1-x}Mn_xTe$, with a comparison to other SnTe alloys [26]. This work not only shows a record peak zT but also a high zT_{ave} in alloy phase.

Acknowledgments

This work is supported by the National Natural Science Foundation of China (Grant No. 51422208, 11474219 and 51401147), the national Recruitment Program of Global Youth Experts (1000 Plan), the program for professor of special appointment (Eastern Scholar) at Shanghai Institutions of Higher Learning, the Pujiang Project of Shanghai Science and Technology Commission (13PJ1408400) and the Bayer-Tongji Eco-Construction & Material Academy (TB20140001).

References

[1] Abelson RD. Space missions and applications. In: Rowe DM, editor. Thermoelectrics handbook : macro to nano. Boca Raton: CRC/Taylor & Francis; 2006. p. 1–7.
[2] Ioffe AF. Semiconductor thermoelements, and thermoelectric cooling. London: Infosearch; 1957.
[3] Fu C, Bai S, Liu Y, Tang Y, Chen L, Zhao X, et al. Realizing high figure of merit in heavy-band p-type half-Heusler thermoelectric materials. Nat Commun 2015;6.
[4] Hsu KF, Loo S, Guo F, Chen W, Dyck JS, Uher C, et al. Cubic $AgPb_mSbTe_{2+m}$: bulk thermoelectric materials with high figure of Merit. Science 2004;303:818–21.
[5] Biswas K, He JQ, Blum ID, Wu CI, Hogan TP, Seidman DN, et al. High-performance bulk thermoelectrics with all-scale hierarchical architectures. Nature 2012;489:414–8.
[6] Poudel B, Hao Q, Ma Y, Lan YC, Minnich A, Yu B, et al. High-thermoelectric performance of nanostructured bismuth antimony telluride bulk alloys. Science 2008;320:634–8.
[7] Pei Y, Lensch-Falk J, Toberer ES, Medlin DL, Snyder GJ. High thermoelectric performance in PbTe due to large nanoscale Ag_2Te precipitates and La doping. Adv Funct Mater 2011;21:241–9.
[8] Kim SI, Lee KH, Mun HA, Kim HS, Hwang SW, Roh JW, et al. Dense dislocation arrays embedded in grain boundaries for high-performance bulk thermoelectrics. Science 2015;348:109–14.
[9] Hochbaum AI, Chen RK, Delgado RD, Liang W, Garnett EC, Najarian Mark, et al. Enhanced thermoelectric performance of rough silicon nanowires. Nature 2008;451:163–7.
[10] Snyder GJ, Toberer ES. Complex thermoelectric materials. Nat Mater 2008;7:105–14.
[11] Chen G, Dresselhaus MS, Fleurial J-P, Caillat T. Recent developments in thermoelectric materials. Int Mater Rev 2003;48:45–66.
[12] Venkatasubramanian R, Siivola E, Colpitts T, O'Quinn B. Thin-film thermoelectric devices with high room-temperature figures of merit. Nature 2001;413:597–602.
[13] Vineis C, Shakouri A, Majumdar A, Kanatzidis M. Nanostructured thermoelectrics: big efficiency gains from small features. Adv Mater 2010;22:3970–80.
[14] Zhao L-D, Lo S-H, Zhang Y, Sun H, Tan G, Uher C, et al. Ultralow thermal conductivity and high thermoelectric figure of merit in SnSe crystals. Nature 2014;508:373–7.
[15] Morelli DT, Jovovic V, Heremans JP. Intrinsically minimal Thermal conductivity in cubic i-V-VI_{2} semiconductors. Phys Rev Lett 2008;101:035901.
[16] Liu H, Shi X, Xu F, Zhang L, Zhang W. Copper ion liquid-like thermoelectrics. Nat Mater 2012;11:422–5.
[17] Zhang WQ. P Natl Acad Sci U. S. A 2014;111:15031–5.
[18] Cahill DG, Watson SK, Pohl RO. Lower limit to the thermal conductivity of disordered crystals. Phys Rev B 1992;46:6131.
[19] Pei Y, Wang H, Snyder GJ. Band engineering of thermoelectric materials. Adv Mater 2012;24:6125–35.
[20] Heremans JP, Jovovic V, Toberer ES, Saramat A, Kurosaki K, Charoenphakdee A, et al. Enhancement of thermoelectric efficiency in PbTe by distortion of the electronic density of states. Science 2008;321:554–7.
[21] Pei Y, Shi X, LaLonde A, Wang H, Chen L, Snyder GJ. Convergence of electronic bands for high performance bulk thermoelectrics. Nature 2011;473:66–9.
[22] Liu W, Tan XJ, Yin K, Liu H, Tang X, Shi J, et al. Convergence of conduction bands as a means of enhancing thermoelectric performance of n-type $Mg_2Si_{1-x}Sn_x$ solid solutions. Phys Rev Lett 2012;108. 166601-(1-5).
[23] Liu WS, Kim HS, Chen S, Jie Q, Lv B, Yao M, et al. n-type thermoelectric material $Mg_2Sn_{0.75}Ge_{0.25}$ for high power generation. P Natl Acad Sci U. S. A 2015;112:3269–74.
[24] Fu CG, Zhu TJ, Pei YZ, Xie H, Wang H, Snyder GJ, et al. High band degeneracy contributes to high thermoelectric performance in p-type half-Heusler compounds. Adv Energy Mater 2014;4(18).
[25] Heremans JP, Wiendlocha B, Chamoire AM. Resonant levels in bulk thermoelectric semiconductors. Energy Environ Sci 2012;5:5510–30.
[26] Tan G, Shi F, Hao S, Chi H, Zhao LD, Uher C, et al. Codoping in SnTe: enhancement of thermoelectric performance through synergy of resonance levels and band convergence. J Am Chem Soc 2015;137:5100–12.
[27] Zhang Q, Liao BL, Lan YC, Lukas K, Liu WS, Esfarjani K, et al. High thermoelectric performance by resonant dopant indium in nanostructured SnTe. P Natl Acad Sci U. S. A 2013;110:13261–6.
[28] Zhang Q, Wang H, Liu W, Wang H, Yu B, Zhang Q, et al. Enhancement of thermoelectric figure-of-merit by resonant states of aluminium doping in lead selenide. Energy Environ Sci 2012;5:5246–51.
[29] Pei Y, Wang H, Gibbs ZM, LaLonde AD, Snyder GJ. Thermopower enhancement in $Pb_{1-x}Mn_xTe$ alloys and its effect on thermoelectric efficiency. NPG Asia Mater 2012;4:e28.
[30] Pei Y, LaLonde AD, Heinz NA, Shi X, Iwanaga S, Wang H, et al. Stabilizing the optimal carrier concentration for high thermoelectric efficiency. Adv Mater 2011;23:5674–8.

[31] Pei Y, LaLonde AD, Heinz NA, Snyder GJ. High thermoelectric figure of Merit in PbTe alloys demonstrated in PbTe−CdTe. Adv Energy Mater 2012;2:670−5.
[32] Ravich YI, Efimova BA, Smirnov IA. Semiconducting Lead Chalcogenides. New York: Plenum Press; 1970.
[33] Nimtz G, Schlicht B. Narrow-gap lead salts. Springer Tracts Mod Phys 1983;98:1−117.
[34] Ravich YI. Basic physical features of the lead chalcogenides. In: Khokhlov D, editor. Lead chalcogenides: physics and applications. New York: Taylor & Fransics Group; 2003. p. 1−34.
[35] Allgaier RS. Valence bands in Lead Telluride. J Appl Phys 1961;32:2185−9.
[36] Crocker AJ, Rogers LM. Valence band structure of PbTe. J Phys Colloq 1968;29. C4 129−32.
[37] Andreev AA, Radionov VN. Determination of band structure of lead telluride from measurements of hall effect at high temperatures. Sov Phys Semicond 1967;1:145−8.
[38] Klemens PG. The scattering of low-frequency lattice waves by static imperfections. Proc Phys Soc 1955;A68:1113−28.
[39] Callaway J, Vonbaeyer HC. Effect of point imperfections on lattice thermal conductivity. Phys Rev 1960;120:1149−54.
[40] Abeles B. Lattice thermal conductivity of disordered semiconductor alloys at high temperatures. Phys Rev 1963;131:1906−11.
[41] Zhao L-D, Dravid VP, Kanatzidis MG. The panoscopic approach to high performance thermoelectrics. Energ Environ Sci 2014;7:251−68.
[42] He J, Kanatzidis MG, Dravid VP. High performance bulk thermoelectrics via a panoscopic approach. Mater Today 2013;16:166−76.
[43] Herman F, Kortum RL, Ortenburger IB, Van Dyke JP. Relativistic band struture of GeTe, SnTe, PbTe, PbSe and PbS. Le J de Physique Colloques 1968;29:62−77.
[44] Veis AN, Ukhanov YI. Study of the absorption coefficient of p-type PbTe. Sov Phys Semicond 1976;10:780−3.
[45] Rogers L. light hole mobility in PbTe:Na. J Phys D Appl Phys 1968;1:1067.
[46] Chernik I, Efimova B, Kaidanov V, Moizhes B. Band model of SnTe(Tin telluride electric properties analysis for verifying semiconductor model with two valence bands in connection with hall effect dependence on temperature). Sov Phys Sol State 1966;7:2032−4.
[47] Zhou M, Gibbs ZM, Wang H, Han YM, Xin CN, Li LF, et al. Optimization of thermoelectric efficiency in SnTe: the case for the light band. Phys Chem Chem Phys 2014;16:20741−8.
[48] Banik A, Shenoy US, Anand S, Waghmare UV, Biswas K. Mg alloying in SnTe facilitates valence band convergence and optimizes thermoelectric properties. Chem Mater 2015;27:581−7.
[49] Tan GJ, Zhao LD, Shi FY, Doak JW, Lo SH, Sun H, et al. High thermoelectric performance of p-type SnTe via a synergistic band engineering and nanostructuring approach. J Am Chem Soc 2014;136:7006−17.
[50] Tan GJ, Shi FY, Doak JW, Sun H, Zhao LD, Wang PL, et al. Extraordinary role of Hg in enhancing the thermoelectric performance of p-type SnTe. Energ Environ Sci 2015;8:267−77.
[51] Han MK, Androulakis J, Kim SJ, Kanatzidis MG. Lead-Free thermoelectrics: high figure of Merit in p-type AgSnmSbTem+2. Adv Energy Mater 2012;2:157−61.
[52] Dudkin L, Gaidukova V, Ostrovskaya L. Issledovaniya tverdikh rastvorov (Sn, Mn) Te. Neorganicheskie Mater 1971;7:1503−6.
[53] LaLonde AD, Ikeda T, Snyder GJ. Rapid consolidation of powdered materials by induction hot pressing. Rev Sci Instrum 2011;82:025104.
[54] Zhou ZH, Uher C. Apparatus for seebeck coefficient and electrical resistivity measurements of bulk thermoelectric materials at high temperature. Rev Sci Instrum 2005;76:023901.
[55] Pei Y, LaLonde AD, Wang H, Snyder GJ. Low effective mass leading to high thermoelectric performance. Energ Environ Sci 2012;5:7963−9.
[56] Pei Y, May AF, Snyder GJ. Self-tuning the carrier concentration of PbTe/Ag_2Te composites with excess Ag for high thermoelectric performance. Adv Energy Mater 2011;1:291−6.
[57] Pei Y, LaLonde A, Iwanaga S, Snyder GJ. High thermoelectric figure of merit in heavy-hole dominated PbTe. Energ Environ Sci 2011;4:2085−9.
[58] Blachnik R, Igel R. Thermodynamic properties of IV-VI compounds lead chalcogenides. Z Naturforsch B 1974;29:625−9.
[59] Perdew JP, Burke K, Ernzerhof M. Generalized gradient approximation made simple. Phys Rev Lett 1996;77:3865.
[60] Kresse G, Furthmüller J. Efficient iterative schemes for ab initio total-energy calculations using a plane-wave basis set. Phys Rev B 1996;54:11169.
[61] Kresse G, Joubert D. From ultrasoft pseudopotentials to the projector augmented-wave method. Phys Rev B 1999;59:1758.
[62] Monkhorst HJ, Pack JD. Special points for Brillouin-zone integrations. Phys Rev B 1976;13:5188.
[63] Leung CH, Vlack LH. Solubility limits in binary (Ca, Mn) chalcogenides. J Am Ceram Soc 1979;62:613−6.
[64] Andreev A. Parameters of a model of two valence bands for SnTe from measurements of the hall effect at high temperatures. Sov Phys Solid State NOV 1967:1232−3. 9,−5−.
[65] Andreev AA. The band edge structure of the IV-VI semiconductors. J de Physique Colloques 1968;29:50−61.
[66] Chernik IA, Kaidanov VI, Vinogradova MI, Kolomoets NV. Investigation of the valence band of lead telluride using transport phenomena. Sov Phys Semicond 1968;2:645−51.
[67] Rogers L. Valence band structure of SnTe. J Phys D Appl Phys 1968;1:845.
[68] Brebrick R, Strauss A. Anomalous thermoelectric power as evidence for two-valence bands in SnTe. Phys Rev 1963;131:104.
[69] Pei YZ, Gibbs ZM, Gloskovskii A, Balke B, Zeier WG, Snyder GJ. Optimum carrier concentration in n-type PbTe thermoelectrics. Adv Energy Mater 2014;4.
[70] Nordheim L. Ann Phys 1931;401:607−40.
[71] Brooks H. Advances in electronics and electron physics, Vol. 7. New York: Academic; 1955. p. 85.
[72] Herman F, Glicksman M, Parmenter R. Progress in semiconductors, Vol. 2. London: Heywood; 1957.
[73] May AF, Toberer ES, Saramat A, Snyder GJ. Characterization and analysis of thermoelectric transport in n-type $Ba_8Ga_{16-x}Ge_{30+x}$. Phys Rev B 2009;80.
[74] Ahmad S, Mahanti SD. Model on L and conductivity for PbTe−multi scattering and nonparabolic band. Phys Rev B 2010;81:165203.
[75] Alekseeva GT, Efimova B, Ostrovsk LM, Serebrya OS, Tsypin M. Thermal conductivity of solid solutions based on lead telluride. Sov Phys Semicond 1971;4:1122−5.

Dr. Wen Li, Tongji University, Email: liwen@tongji.edu.cn. Wen Li is an assistant researcher at Tongji University, China.His research is focused on developing new thermoelectric materials and understanding the material parameters that determine the thermoelectric properties, as well as engineering of these parameters for further enhancement of performance. He received a M.E. and a B.E. both from Zhengzhou University, China and a Ph. D from Shizuoka University, Japan.

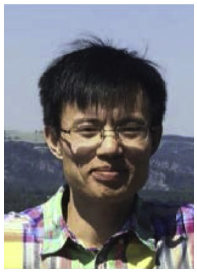

Professor Yanzhong Pei, Tongji University, Email: yanzhong@tongji.edu.cn. Yanzhong Pei is a professor at Tongji University, China. He has been working on advanced thermoelectric semiconductors for about a decade, from synthesizing the materials to understanding the underlying physics and chemistry. He holds a B.E. from Central South University in China, a Ph. D from Shanghai Institute of Ceramics, CAS and postdoctoral research experience from Michigan State University and the California Institute of Technology. He has so far published about 50 papers, which receive a total citation over 2000.